Articles presented during:

XIX Krajowa Konferencja Mechaniki Płynów
19th Polish Fluid Dynamics Conference

POZNAŃ

05-09.09.2010

FLOW FOCUSING IN MICROFLUIDIC DEVICES

Slawomir Blonski[1], *Piotr Domagalski*[2,3,4], *Tomasz A. Kowalewski*[1]

[1] Institute of Fundamental Technological Research, Polish Academy of Sciences, Warsaw, Poland
sblonski@ippt.gov.pl; tkowale@ippt.gov.pl

[2] Faculty of Process and Environmental Engineering, Technical University of Lodz, Łódź, Poland
[3] Department of Process and Energy, Delft University of Technology, Delft, The Netherlands
[4] Department of Biotechnology, Delft University of Technology, Delft, The Netherlands
P.M.Domagalski@tudelft.nl

Abstract

This paper presents numerical analysis of the hydrodynamic flow focusing in rectangular microchannels. The low Reynolds number pressure driven flow in symmetric system of crossed channels with three inlets and one outlet is investigated. The numerical model is used to elucidate the origin of broadening of the focused flow sheet observed experimentally close to the side walls of the outlet channel. It is found that the observed broadening is mainly due to the residual flow inertia and can be totally eliminated if flow Reynolds number is less than one.

1. Introduction

The advances of microfluidic technology have led to development of miniaturized devices for manipulating and sorting bio-samples, mixing and delivering chemical reagents, or encapsulating immiscible liquids. In most cases these devices use either simple T-shaped channels with two inlets side-by-side and one outlet or two crossed channels with three inlets and one outlet. Mixing properties of such devices are often crucial for the effective functioning of microfluidic devices [1; 2]. Due to the smallness of the devices the flow Reynolds number is small and only molecular diffusion is responsible for the inter-diffusion of reagents [3]. This very slow process can be accelerated by increasing contact surface between two reacting liquid streams or by introducing flow instability leading to its chaotic behaviour [4; 5; 6].

There is class of microfluidic systems where flow mixing should be minimized. An example is so called flow focusing process [7; 8; 9], where the sample flow (supplied from the inlet channel) is constrained laterally within the centre of the microchannel by two neighbouring sheath flows from the side channels (see Fig.1). In symmetric hydrodynamic focusing, the sample flow is constrained by two sheath flows to a thin sheet at the channel symmetry. By manipulating flow rates of the focusing flows location of the focused sheet can be moved out of the symmetry plane. Achieving a precise control of the focused stream width is crucial in various applications of the flow focusing systems.

Due to the fabrication constrains such devices usually use straight channels of rectangular cross-section, of typically 50 to 100μm and 5-10mm length interconnected at right angles. The flow velocity in the microchannels is less than 1mm/s, generally regarded as laminar, low Reynolds number flow. Hence, it is assumed that flow streamlines remain parallel and mixing of liquids is mostly controlled by diffusion. However, even for very low Reynolds number regime the abrupt change of the flow direction when fluid passes T-junction appears to produce secondary flow forcing fluid to move towards side walls. It strongly affects both mixing as well as flow focusing efficiency. The effect is caused by two well know mechanisms, so called Moffat-eddies, created by the flow passing sharp corners, and Dean flow – secondary circulation generated due to the flow curvature. Both mechanisms, present even for very low Reynolds number flow evidently change flow pattern and species distribution observed in the outlet channel. Experimentally it is observed as broadening of the flow-focusing especially in the regions close to the side walls. The effect is important for the effectiveness of microfluidic devices and has to be considered by selecting proper flow regimes for working device.

Here, we investigate numerically evolution of the flow structure with variation of the flow Reynolds number from 0.1 to 100 for the simple flow-focusing device to elucidate influence of flow parameters on its performance. The geometry of the device used is that from the experiment described elsewhere [10; 11], where we demonstrated possibility for improving micro-PIV measurements by flow-focusing of the seeding particles.

2. Experimental

A polymeric device was fabricated to visualize performance of the flow focusing device. The device was made of 5mm thick polymethylmethacrylate (PMMA) and consists of two crossed rectangular channels of $300\mu m \times 420\mu m$ cross section made by micro milling. A small ($90\mu m \times 90\mu m$) protrusion was made 5mm downstream on the bottom wall of the outlet channel to monitor stability of the focused sheet.

The flow was analysed using microPIV [12; 13] system built on Nikon Eclipse E-50i epi-fluorescent microscope, long working distance objective 10x/0.3 WD 17.5 (Nikon LU PLAN FLUOR) and SensiCam Double Shutter 12-bit CCD camera with resolution 1280×1024 pixels (PCO IMAGING). The illumination was provided by SoloPIV Nd:YAG pulsed laser (532nm) from New Wave Research Inc. The flow was forced by syringe pumps (New Era Pump Systems Inc.). The flow rate was maintained between $1.46 \cdot 10^{-4}\, ml/h$ and $1.87 \cdot 10^{-2}\, ml/h$, what corresponds with Reynolds number $Re_{min} = 0.48$ and $Re_{max} = 62$. The flow rate ratio of the focusing stream to the focused flow was set to 20:1 guarantying stable, about 15μm thin sheet of focused flow.

Deionised water and fluorescent tracers (Fluorescent Polymer Microspheres 2μm, Duke Sci.) were used as media.

Fluorescent tracers were present in the focused stream and they concentration monitored by the camera. Particle tracing was applied to visualise flow structure at the crossing area of the focusing device (Fig. 2).

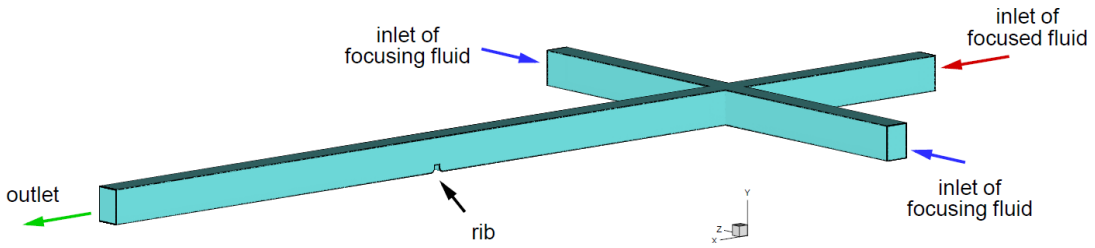

Figure 1: *Geometry of the flow focusing microfluidics device*

Our experimental investigations indicated that focused flow sheet is not necessarily uniform and its thickening close to the walls may reach undesirable value [14]. Three dimensional study of this effect performed by using confocal microscopy (Fig. 3) confirmed that focused sheet is not flat and with increasing flow rate it exhibits nearly tripled thickness at both side walls (Fig. 3c).

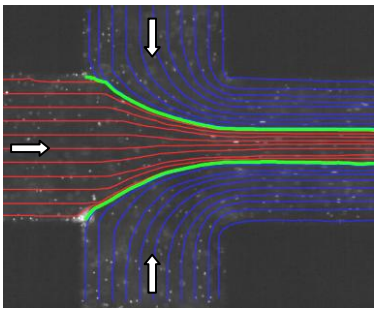

Figure 2: *Particle tracking applied to fluorescent particle tracers observed in the flow-focusing microfluidic device; tracers are present both in focusing and focused flow*

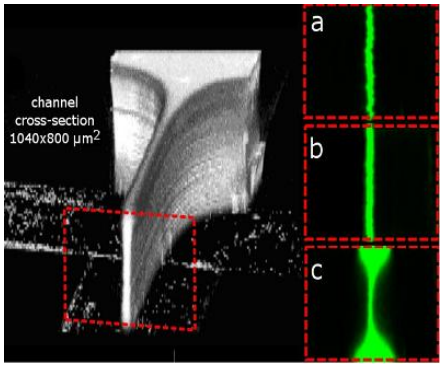

Figure 3: *Flow focusing observed under confocal microscope; a, b, c - thickening of the focused plane closed to the side walls observed when increasing flow rate (Reynolds number equal 3.23, 6.46 and 12.92, respectively)* [15]

Local thickening of the focused plane is strongly undesirably. It limits efficiency of devices used for sorting purposes or changes reaction rate across the outlet channel, if it is used as a chemical reactor. In our experiments [10; 11] flow focusing of seeding particles was used to improve performance of the microPIV flow analysis [16; 17]. Undesired thickening of the focused sheet including tracers effectively decreased accuracy of the PIV evaluation close to the wall [11]. In the following numerical study we aim to analyse main futures of the flow focusing device and to extract factors responsible for the observed deterioration of the focused flow sheet.

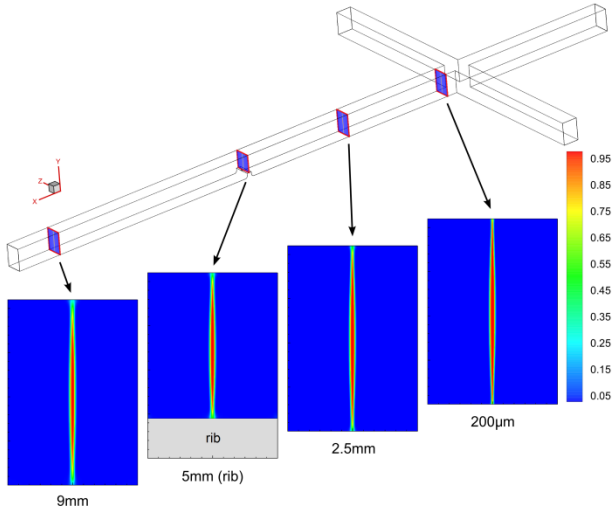

Figure 4: *Flow focusing obtained from numerical model for Reynolds number 0.4. Ratio of the flow rate from side inlets relative to the focused inlet is 20. Despite long distance traveled through the outlet channel and presence of the obstacle located on the way, thickness of the focused sheet remains all the way constant and equals about 17μm*

3. Numerical analysis

The steady, laminar and isothermal flow of viscous incompressible liquid is analyzed using finite volume code Fluent 12 (Ansys Inc) [18]. A three-dimensional (3-D) mesh representing the flow focusing device used in the experiment was built using Gambit 2.6 (Fluent Inc). The geometry and dimensions of the CFD model were identical to the experimental device. The boundary conditions were set as a mass flow at the inlets and as pressure at the outlet. Different meshes were tested until mesh refining had little effect on the computations results. Finally several simulations were performed with the structural hexahedron mesh of over 11

mill cells by varying flow rate to cover Reynolds number[1] from 0.1 to 100.

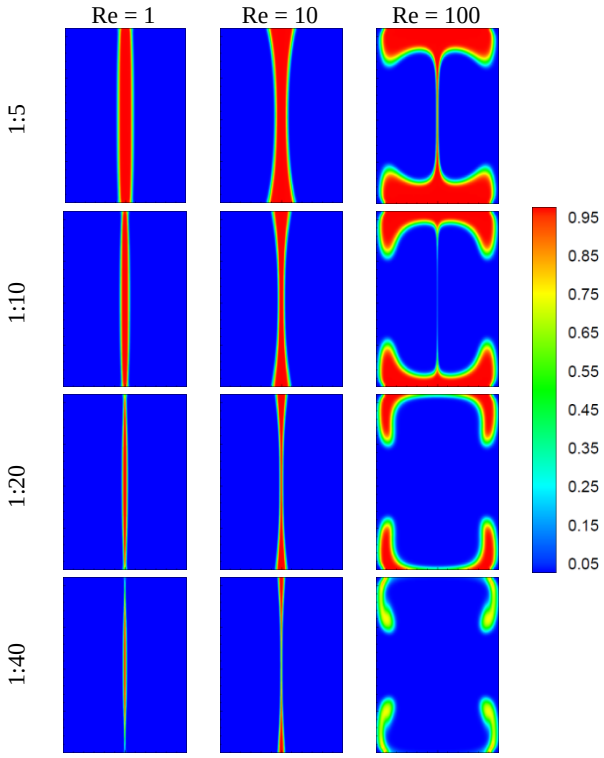

Figure 5: *Mass fraction distribution of the focused fluid for different flow Reynolds numbers (columns) and different focused:focusing fluids flow rate ratios (rows)*

In the experiment the focusing performance of the system was analyzed by introducing small (2μm) florescent particles to the focused liquid and observing their concentration in the outlet channel. In the numerical model to determine flow structure and shape of the focused layer containing fluorescent tracer particles we used non-reacting species transport model with two liquids having the same physical and chemical properties (pure water without particles). To provide proper mixing conditions of the focused and focusing fluids and appropriate migration velocity of the tracer particles, the mass diffusivity coefficient of the liquid was set to be $2.22 \cdot 10^{-13}\, m^2/s$, equal to the diffusivity of dilute water solution of spherical particles used as seeding [19]. Figure 4 demonstrates numerical simulation of the focusing effect obtained for the Reynolds number equal 0.4.

It is evident that thickness of the focused plane remains practically constant over long distance from the crossing region of inlet channels. Obviously diffusion of investigated solution of particles is negligible small. Even after passing the obstacle (see Fig. 4) made at the bottom wall undisturbed sheet of the focused flow is fully recovered. Small diffusivity of particles confirms rough estimation of the diffusion distance based on the diffusion constant and flow velocity, indicating that on their way down the flow particles may diffuse distance of less than 0.1μm.

Numerical simulation performed for four different ratios of the inlet flow rate indicates that thickness of the focused plane decreases with increase flow rate ratio (Fig. 5). However, very strong effect on the focused sheet structure is observed by varying total flow rate, i.e. the flow Reynolds number (Fig. 5 and 6). Increasing Reynolds number above 10 practically destroys flow focusing mechanism and for Reynolds number above 50 focused fluid is fully layered on the side walls being absent in the channel center.

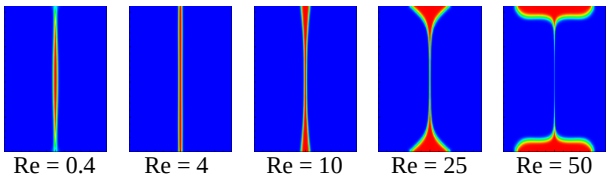

Figure 6. *Mass fraction distribution of the focused fluid in the channel cross-section calculated for Re=0.1, Re=4, Re=10, Re=25 and Re=50. Ratio of flow rates equals 20*

Numerical simulations clearly indicate three regimes of the flow focusing:

- Regular, well defined, nearly flat focused plane can be obtained for Reynolds number 4. Smaller Reynolds number creates slightly convex shape.
- Double concave shape is present for Reynolds number above 10
- Complete layering of the focused flow on the side walls takes place for Reynolds number approaching 100.

Numerical analysis indicates that the source of the observed disturbances is located in small region where three streams merge together to the outlet channel. It is worth to repeat that molecular diffusion is completely negligible for analysed case. Hence, the geometry of the focused plane once created by three merging streams remains unchanged along the outlet channel. For low flow Reynolds number there are only two possible mechanisms responsible for observed deformation of the focusing plane, so called Moffat-eddies [20], created by the flow passing sharp corners, and Dean flow – secondary circulation generated due to the flow curvature [21; 22]. Both mechanisms are responsible for deformation of the velocity pattern, visible on Figure 7 and 8. It can be seen that both transversal velocity components responsible for the secondary flow increase over 30-times their relative value for higher Reynolds number. We may note concentration of the secondary flow into well visible spots in four corners of the channel. The cross flow found in the corners is responsible for the lateral transport of liquid and effectively for broadening of the focused sheet at the top and bottom walls.

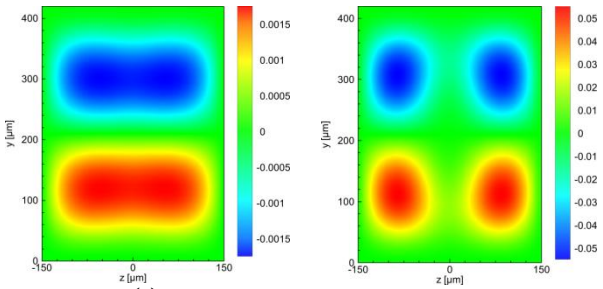

(a) (b)

Figure 7. *Normalized y-component of the velocity (by mean velocity) in the plane 200μm behind the channels crossing for two Reynolds numbers : (a) Re=0.4, (b) Re=25*

[1] Reynolds number is based on the mean outlet flow velocity and outlet channel geometry (hydraulic diameter).

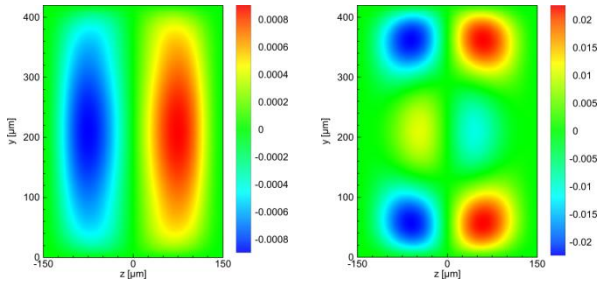

(a) (b)

Figure 8. *Normalized z-component of the velocity (by mean velocity) in the plane 200µm behind the channels crossing for two Reynolds numbers: (a) Re=0.4, (b) Re=25*

Figure 9 collects results of the numerical investigations by displaying normalized cross flow velocity as a function of distance and Reynolds number. One may find that strong lateral flow components are present only at the vicinity of the crossing area. It is the place were the main redistribution of particle concentration takes place. At larger distances (over 1mm, i.e. 3 channel diameters) the parabolic flow profile is established preserving disturbed concentration distribution. The effect of Reynolds number is clearly visible, the relative value of the lateral flow increases with Reynolds number and its presence decreases with the distance.

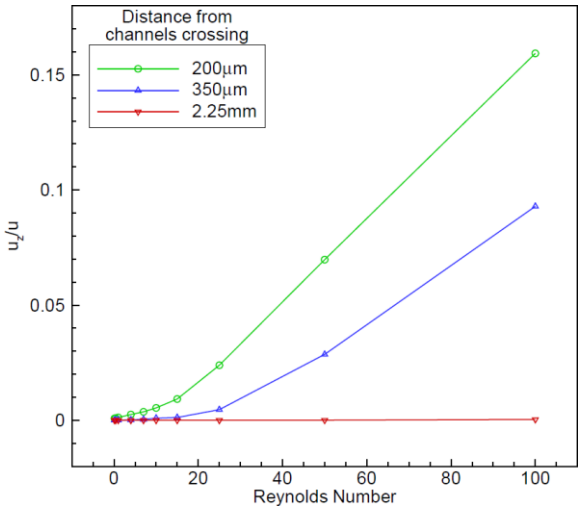

Figure 9. *Normalized (by mean velocity) maximum value of the z-component of the velocity vs. Reynolds number for different distances from channels crossing*

4. Conclusions

Flow structure for the simple flow-focusing device is evaluated to elucidate influence of flow parameters on its performance. The performed parametric study shows that increasing flow Reynolds number from 1 to 10 results in nearly doubled thickness of the focused sheet in the wall region. Such broadening was reported in the experiments. Higher flow rates ($Re > 50$) produce nearly flat boundary layer of focused flow covering both top and bottom walls of the outlet channel. The flow patterns analyzed at several cross-sections of the channel indicate multi-cell regions of the secondary flow responsible for the focusing sheet broadening. Information gained from this study will help to optimize geometry of the focusing device and to minimize effect of the secondary flow by avoiding sharp corners and sudden changes of the flow direction.

5. Acknowledgements

The This work was supported by Ministry of Science and Higher Education of Poland as research project Nr N N20829433 “Badanie ogniskowania hydrodynamicznego cieczy w węźle mikrokanałów” and grant no. N501008733 „Intensyfikacja procesu mieszania w mikroprzepływach”.

6. References

[1] J.M. Ottino, S. Wiggins. *Introduction: mixing in microfluidics*. Phil. Trans. R. Soc. Lond. A, 362(1818). pp. 923-935, 2004.

[2] N.T. Nguyen, Z. Wu. *Micro-mixers – a review*. Journal of Micromechanics and Micro-engineering, 15(2). pp. 1-16, 2005.

[3] A.E. Kamholz, P. Yager. *Theoretical analysis of molecular diffusion in pressure-driven laminar flow in microfluidic channels*. Biophysical Journal, 80. pp. 155-160, 2001.

[4] J.M. Ottino. *The art of mixing with an admixture of art: Fluids, solids, and visual imagination*. Physics of Fluids, 22(2). Article Number: 021301, 2010.

[5] J. Szumbarski. *Instability of viscous incompressible flow in a channel with transversely corrugated walls*. Journal of Theoretical and Applied Mechanics, 45(3). pp. 659-683, 2007.

[6] T.A. Kowalewski, J. Szumbarski, S. Blonski. *Low-Reynolds-Number instability of the laminar flow between wavy walls*. Proc. of ASME ICNMM2008. CD-ROM proceedings ISBN 0-7918-3826-9, paper 62070, pp. 1-8, TU Darmstadt, Germany, 2008.

[7] Z. Wu, N.T. Nguyen. *Hydrodynamic focusing in microchannels under consideration of diffusive dispersion: theories and experiments*. Sensors and Actuators B, 107(2). pp. 965-974, 2005.

[8] G.M. Lee, S. Choi, J. Park. *Three-dimensional hydrodynamic focusing with a single sheath flow in a single-layer microfluidic device*. Lab Chip, 9(21). pp. 3155-3160, 2009.

[9] X. Mao, S.S. Lin, C. Dong, T.J. Huang. *Single-layer planar on-chip flow cytometer using microfluidic drifting based three-dimensional (3D) hydrodynamic focusing*. Lab Chip, 9(11). pp. 1583-1589, 2009.

[10] P. Domagalski, M. Dziubinski, S. Blonski, T.A. Kowalewski. *Zastosowanie ogniskowania hydrodynamicznego jako modyfikacji techniki micro-PIV*. I Krajowa Konferencja Nano- i Mikromechaniki. Krasiczyn, 8-12 lipca, 2008.

[11] S. Blonski, P. Domagalski, M. Dziubinski ,T. Kowalewski. *Hydrodynamically modified seeding for micro-PIV*. Archives of Mechanics. Paper to be submitted, 2010.

[12] M. Raffel, C. Willert, J. Kompenhans. *Particle Image Velocimetry: A Practical Guide*. Springer-Verlag. Berlin, 1998.

[13] T.A. Kowalewski, S. Błoński, P. Korczyk. *Eksperymentalna analiza przepływów w skali mikro i nano. Wybrane zagadnienia przepływu płynów i wymiany ciepła*. Praca zbiorowa pod redakcją W. Sucheckiego, pp. 127-149, Oficyna Wydawnicza Politechniki Warszawskiej, 2008.

[14] R.F. Ismagilov, A.D. Stroock, P.J.A. Kenis, G. Whitesides, H.A. Stone. *Experimental and theoretical scaling laws for transverse diffusive broadening in two-phase laminar flows in microchannels*. App. Phys. Lett., 76(17). pp. 2376-2378, 2000.

[15] P.M. Domagalski, M. Dziubinski, P. Budzynski, M.M. Mielnik, L.R. Saetran. *Width variations of hydrodynamically focused streams in low to moderate Reynolds number*. Proceedings of European Conference of Chemical Engineering (ECCE-6), Kopenhagen, Denmark, September, 2007

[16] M.M. Mielnik, L.R. Saetran. *Selective seeding for micro-PIV*. Experiments in Fluids, 41(2). pp. 155-159, 2006.

[17] P.M. Domagalski, M.M. Mielnik, I. Lunde, L.R. Saetran. *Characteristics of Hydrodynamically Focused Streams for Use in Microscale Particle Image Velocimetry (Micro-PIV)*. International Journal of Heat Transfer Engineering, 28(8). pp. 680-688, 2008.

[18] Fluent 12. User's Guide. ANSYS Inc. 2010.

[19] A. Einstein. *On the movement of small particles suspended in a stationary liquid demanded by the molecular-kinetic theory of heat*. Theory of the Brownian Movement. Dover Publications Inc, New York, pp. 1-18, 1905.

[20] H.K. Moffatt. *Viscous and resistive eddies near a sharp corner*. J. Fluid Mech., 18. pp. 1-18, 1964.

[21] S. Kim, S.J. Lee. *Measurement of Dean flow in a curved micro-tube using micro digital holographic particle tracking velocimetry*. Exp Fluids, 46(2). pp. 255-264, 2009.

[22] K. Yamamoto, X. Wu, K. Nozaki, Y. Hayamizu. *Visualization of Taylor-Dean flow in a curved duct of square cross-section*. Fluid Dynamics Research, 38. pp. 1-18, 2006.